Applied Surface Science 466 (2019) 126–132

Contents lists available at ScienceDirect

Applied Surface Science

journal homepage: www.elsevier.com/locate/apsusc

Full Length Article

Robust $Mg(OH)_2$/epoxy resin superhydrophobic coating applied to composite insulators

Wenyu Peng[a,c], Xuelian Gou[b,c], Hongling Qin[a,*], Meiyun Zhao[a], Xinze Zhao[a], Zhiguang Guo[b,c,*]

[a] College of Mechanical and Power Engineering of China Three Gorges University, Yichang 443002, People's Republic of China
[b] Hubei Collaborative Innovation Centre for Advanced Organic Chemical Materials and Ministry of Education Key Laboratory for the Green Preparation and Application of Functional Materials, Hubei University, Wuhan 430062, People's Republic of China
[c] State Key Laboratory of Solid Lubrication, Lanzhou Institute of Chemical Physics, Chinese Academy of Sciences, Lanzhou 730000, People's Republic of China

ARTICLE INFO

Keywords:
Superhydrophobic
Composite insulators
Robust coating
Mechanical stability
Anti-voltage ability

ABSTRACT

Composite insulators with superhydrophobic coatings can ensure the safe operation of railways, electricity and telecommunication systems. A robust $Mg(OH)_2$/epoxy resin superhydrophobic coating for composite insulators is reported. The coating is fabricated by a simple method, and the water contact angle reaches its maximum value of 155° at the stearic acid loading of 0.285 g. The superhydrophobic property is controlled by different amounts of stearic acid, which influence the surface roughness of the coating. Additionally, the coating shows mechanical stability, chemical durability and a self-cleaning property, allowing it to be stored in water for more than 20 days. In consideration of the above-mentioned advantages, these characteristics make the composite insulators with this coating a better value than the commercial composite insulators, which is of great benefit to global electricity issues.

1. Introduction

The composite insulator is a universal and essential component for use in transmission lines due to its low cost and light weight [1,2]. However, it has often been damaged by environmental pollution, fouling, icing and corrosive treatment leading to electricity outages and even tower collapse. The property of superhydrophobicity is crucial for composite insulators, not only to prevent liquid from contacting the surface of the composite insulator but also to improve global electricity and telecommunication systems. Moreover, composite insulators with the proposed superhydrophobic coating can reduce tremendous economic damage.

Conventionally, superhydrophobicity is defined as possessing a water contact angle (CA) larger than 150° and a sliding angle (SA) less than 5° [3–6]. In recent decades, superhydrophobic materials have undergone intense research and become a significant part of various industrial areas including automobile windshields, oil-water separation, water collection and antibacterial applications [7–12]. In general, complicated processes such as etching [13], template use [14] and chemical vapour deposition [15] are involved in order to create artificial superhydrophobic surfaces for various needs. Superhydrophobic coatings were developed with a focus on the roughness and low surface energy of the material. Meanwhile, a few studies have been performed on the application of superhydrophobicity for composite insulators. For example, Zuo et al. [16] fabricated a superhydrophobic surface with ZnO nanorods through a radio frequency magneton sputtering method, which showed great superhydrophobicity with a CA of 167.1° and a SA of 2°. However, it was limited by various drawbacks, such as its high cost as well as complicated and toxic preparation processes. Accordingly, Cao et al. reported synthetic $Mg(OH)_2$ (MH) nanostructures via a biomolecule-assisted hydrothermal route [17]. The surface showed a self-cleaning property based on its superhydrophobicity, with contact angles larger than 150° and sliding angles less than 3°. However, this process could not exhibit mechanical stability, such as passing a simple abrasion test or a mechanical friction test. Li et al. [18] prepared a superhydrophobic coating on glass/porcelain insulators. Although the coating showed an anti-icing property below the freezing temperature, this method was expensive and complicated. Besides, impacting the anti-voltage property may be crucial for the composite insulators used in the fields of railways and telecommunication systems. In consideration of simple methods and practical applications, the application of robust $Mg(OH)_2$/epoxy resin superhydrophobic coatings to composite insulators is still a challenge.

In this work, a green and facile method was proposed to achieve Mg

* Corresponding authors at: State Key Laboratory of Solid Lubrication, Lanzhou Institute of Chemical Physics, Chinese Academy of Sciences, Lanzhou 730000, People's Republic of China (Z. Guo).
E-mail addresses: qhl1120@qq.com (H. Qin), zguo@licp.cas.cn (Z. Guo).

https://doi.org/10.1016/j.apsusc.2018.10.039
Received 7 August 2018; Received in revised form 26 September 2018; Accepted 4 October 2018
Available online 05 October 2018
0169-4332/

$(OH)_2$/epoxy resin superhydrophobic coatings for composite insulators. The coatings were nontoxic and possessed a low surface energy after modification by stearic acid (STA). The epoxy resin showed a high adhesive force and good binding capability [19–22]. The coating not only displayed excellent superhydrophobicity with a low adhesive force and roughness but also possessed multifunctional abilities such as anti-voltage, self-cleaning, antifouling, anti-icing, mechanical durability and chemical stability properties. Importantly, the obtained $Mg(OH)_2$/epoxy resin superhydrophobic coatings can reduce electricity loss and satisfy the needs of the power industry.

2. Experimental section

2.1. Materials and chemicals

$MgCl_2{\cdot}6H_2O$ (AR) was obtained from the Tianjing Fengyue Chemical Reagent Co. Inc., China. Stearic acid (STA) was purchased from the Longxi Chemical Reagent Co. Ltd., Shantou, China. Ammonium hydroxide ($NH_3{\cdot}H_2O$) (AR 97%) was obtained from the Henan Xinxiang Zhongyuan Organic Chemical Co. Ltd., China. Polyvinyl pyrrolidone (PVP) was obtained from the Shanghai Kefeng Chemical Reagent Co. Inc. Epoxy resin and curing agent were purchased from the Beijing Yuhong Waterproof Technology Co. Ltd. Sudan red IV, orange II sodium salt and methylene blue were obtained from Aldrich. In addition, all other chemicals were analytical-grade reagents and were used as received.

2.2. Preparation of superhydrophobic powder

First, 2 g of $MgCl_2{\cdot}6H_2O$ and 0.1 g of polyvinyl pyrrolidone (PVP) were added to 100 mL of deionized water and stirred for 30 min. Next, 5 mL of $NH_3{\cdot}H_2O$ and 45 mL of deionized water were added to the above mixture and stirred for 2 h at room temperature. Next, 0.285 g of stearic acid (STA) and 30 mL of ethanol were added into this solution and stirred for 3 h. The mixture was then dried in a vacuum oven at 100 °C for 5 h. The white modified $Mg(OH)_2$ particles were collected through filtration and washed with ethanol twice. Finally, the superhydrophobic powders were obtained and harvested for the subsequent experiment.

2.3. Preparation superhydrophobic coatings on various substrates

Schematic Fig. S1 shows the preparation procedure for the superhydrophobic coating. First, the various substrates, such as fabric, composite insulator, wood and glass, were immersed in a mixture of 0.23 g of curing agent and 0.8 g of epoxy resin for 2 min at room temperature. Then, the modified $Mg(OH)_2$ powders were carefully spread on the coatings via dip-coating and sieve-deposition. Next, the coatings covered with white particles were dried in a vacuum oven at 100 °C for 3 h. Finally, the samples deposited with powders were pressed in order to improve the bonding strength. As presented in Fig. 1, the $Mg(OH)_2$/epoxy resin superhydrophobic coating on various substrates was obtained.

2.4. Characterization

Field emission scanning electron microscopy (FESEM) images were obtained on JSM-6701F instrument using Au-sputtered specimens. The crystal structure was characterized by X-ray diffraction (XRD) using an X'PERT PRO diffractometer with Cu Kα radiation having a 1.5418 Å wavelength with 2θ ranging from 5° to 120°. Transmission electron microscopy (TEM) measurements were carried out with a TechnaiG20 (FEI) instrument operating at 300 kV. Fourier transform infrared spectroscopy (FTIR, Nicolet iS10, Thermo Scientific) was performed, and the spectra were recorded. Three-dimensional surface imaging was carried out using surface imaging system atomic force microscopy (AFM, CSPM 5500). The elemental distribution maps of samples were obtained by energy dispersive spectroscopy (EDS, Kevex). X-ray photoelectron spectroscopy (XPS) (ESCALAB 250Xi, Thermo Scientific) measurements were performed using Al-Kα radiation to analyse the elements and functional groups. The size distribution of particles was measured with a Zetasizer Nano ZS ZEN 3600. The water CAs and SAs were measured (JC2000D) with a 5 μL distilled water droplet at ambient temperature. The average water contact angle and sliding angle values were obtained by measuring the same sample at five different positions. All photographs were obtained by a Sony camera (DSCHX200).

3. Results and discussion

3.1. Surface wettability and morphology

The relationship between the water CA and STA loading on the hydrophobic property of the coating is shown in Fig. 2. Apparently, the water CA of the coating increased from 70° to 155° when the STA loading increased from 0 g to 0.285 g. This indicates that the water CA value of the coating increased with an increasing amount of STA. However, the wettability also changed due to the surface roughness. The SEM images and the TEM images with different STA loadings are shown in Fig. 2a–e and f–j, respectively. The original coating surface was smooth with a CA of 70°, indicating that it possessed hydrophilic wettability (Fig. 2a and f). Obviously, the insets of Fig. 2e and j show that the modified coating has a high water CA (155°) and micro/-nanostructure, as shown in the following equation [17]:

$$Mg(OH)_2 + CH_3(CH_2)_{16}COOH \rightarrow CH_3(CH_2)_{16}COOMg + H_2O \quad (1)$$

As shown in Fig. S3, the three-dimensional AFM images and size distribution of the coating were measured to prove the afore-mentioned observation. It can be observed that it completely consisted of

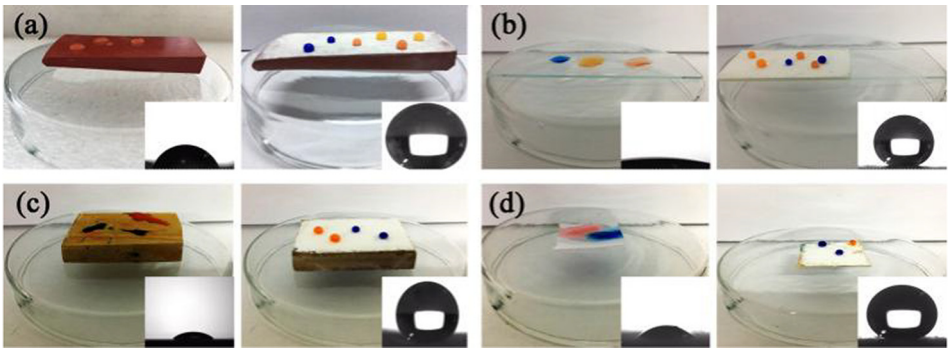

Fig. 1. Photographs of water droplets on four different original substrates (left) and coated substrates (right): (a) composite insulator, (b) glass, (c) wood, (d) fabric, respectively. Shown in the insets are the optical images of the static water droplets (5 μL).

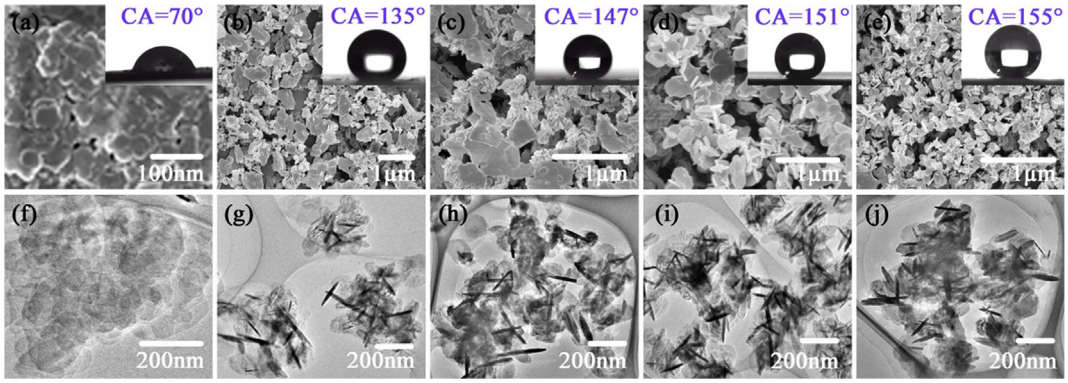

Fig. 2. SEM images of the (a) original $Mg(OH)_2$ coating, (b) SAT-0.036 g, (c) SAT-0.0713 g, (d) SAT-0.143 g, and (e) SAT-0.285 g. TEM images of the (f) original $Mg(OH)_2$ coating, (g) SAT-0.036 g, (h) SAT-0.0713 g, (i) SAT-0.143 g, and (j) SAT-0.285 g. The corresponding optical images of water droplets are shown in the inset (5 μL).

nanowires and exhibited a morphology with an average surface roughness (*Ra*) of approximately 20.03 nm. When the STA loading ranged from 0 g to 0.285 g, the size of the $Mg(OH)_2$ particles was larger. The results show that the radii of pristine $Mg(OH)_2$ particles were less than 200 nm, and the $Mg(OH)_2$ particles modified by STA were larger than 200 nm in diameter (Fig. S3c and d).

To further prove that the surface was modified by STA, analyses were performed using XRD, XPS and FTIR. The diffraction peaks did not change after modification because their XRD (Fig. 2a and d) peak intensities are almost identical. There is a slightly different peak for the modified $Mg(OH)_2$ particles. The (0 0 2) peaks represent $C_{36}H_{70}MgO_4$ and $C_{18}H_{36}O_2$, as shown in Fig. S3. By comparing the XPS patterns of the original $Mg(OH)_2$ particles and the modified $Mg(OH)_2$ particles (Fig. 3b and e), six main characteristic peaks appearing at 1304 eV, 530 eV, 307 eV, 285 eV, 84 eV and 47 eV were observed, which can be attributed to the existence of Mg 1s, O 1s, Mg KL1, C 1s, Mg 2s and Mg 2p, respectively. However, the analysis of the surface elements is a required method to directly demonstrate the changes of the surface chemical composition. The EDS (insets in Fig. 3b and e) found that the proportion of the element Mg decreased from 25.9% to 10.62%, while the proportion of the element C increased from 22.44% to 49.74%, which indicated that the surface was successfully modified by STA. Similarly, Fig. 3c and f show the FTIR spectra of the samples. In curve 3c, the peaks at 3699 cm^{-1} and 3421 cm^{-1} were the antisymmetric stretching vibration peaks of the −OH bonds in the MH group. The adsorption peaks at 2919 cm^{-1} and 2850 cm^{-1} were attributed to the stretching vibrations of C−H in the $-CH_3$ and $-CH_2-$ groups of STA. The peaks at 1577 cm^{-1} and 1467 cm^{-1} were the symmetric stretching vibration peaks of C═O bonds in MH and STA due to the formation of the new chemical bond [23]. It is noted that the adsorption peaks at approximately 1706 cm^{-1} did not appear, which also proved this point [24]. The above results also demonstrate that the STA plays a significant role in the surface roughness and lowing the surface free energy.

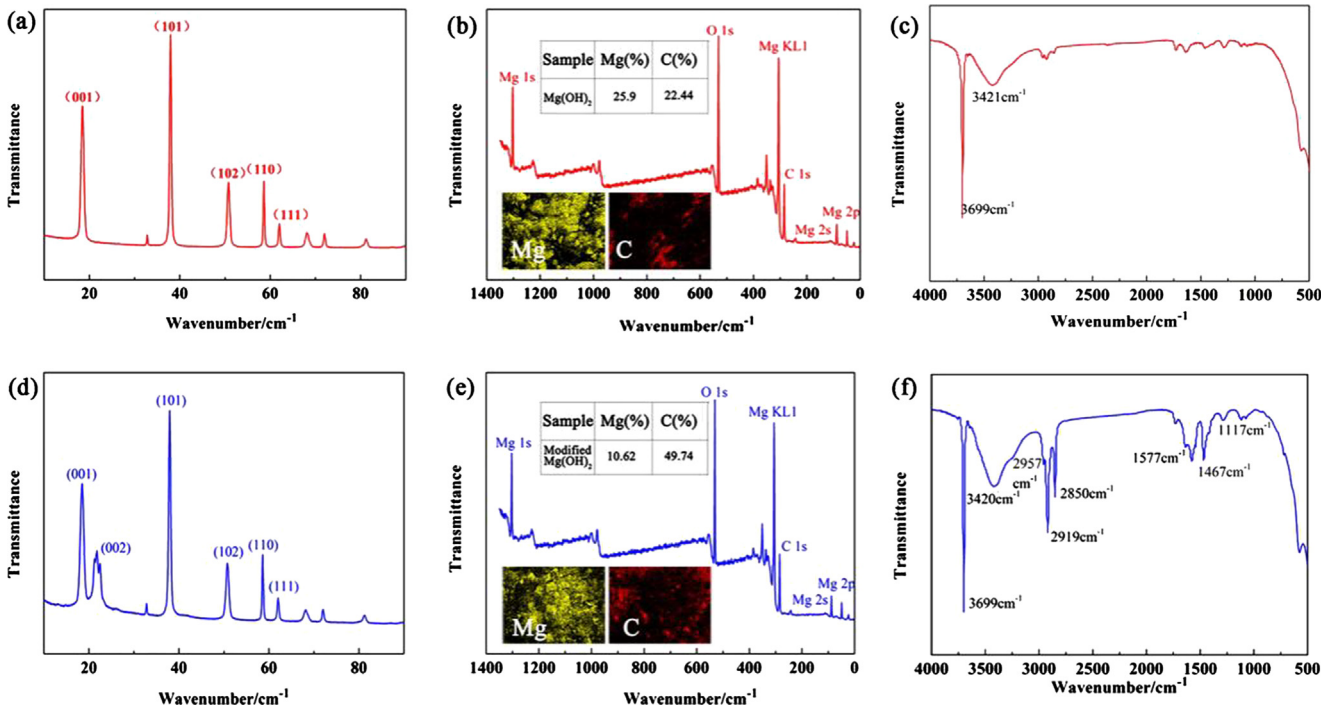

Fig. 3. Characterizations of the original $Mg(OH)_2$ nanoparticles: (a) XRD spectrum, (b) XPS spectrum and EDS maps of Mg and C elements, and (c) FTIR spectrum of the original $Mg(OH)_2$ nanoparticles. (d) XRD spectrum, (e) XPS spectrum and EDS maps of Mg and C elements, and (f) FTIR spectrum of the $Mg(OH)_2$ nanoparticles after modification.

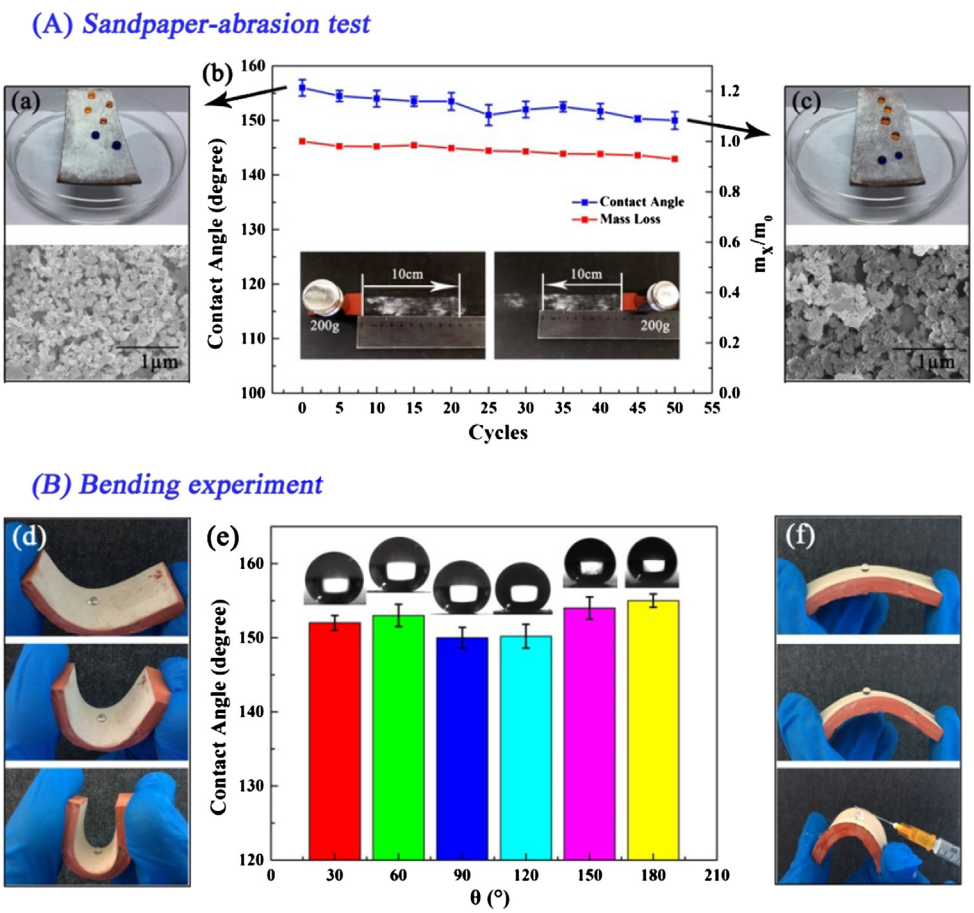

Fig. 4. A: (a) and (c) SEM images before and after 50 abrasion cycles, respectively. (b) Contact angle and mass loss (m_0 and m_x are the mass of the superhydrophobic coating before and after cycles with sandpaper) under 200 g of weight. B: (d) and (f) Photographs of the bending of the coatings. (e) The contact angle of the superhydrophobic coating after bending.

3.2. Mechanical stability

Many superhydrophobic coatings are easily destroyed or removed due to the fine roughness structure and weak mechanics. Therefore, some attempts have been made to increase the mechanical stability of superhydrophobic coatings [25–27]. However, only a few studies have reported the mechanical stability and durability of superhydrophobic coatings for composite insulators. To solve this problem, the as-prepared coating developed in this work can be used for electrical applications.

For the sandpaper-abrasion test, the coating (5 cm × 2 cm) under a 200 g weight was moved for 10 cm along a ruler by an external drawing force and returned back (Movie S1). Fig. 4b demonstrates that the water CAs were all above 150°, and the loss of quantity was approximately 8% after 50 abrasion cycles. On the other hand, it is surprising that there were no obvious changes to the coating before and after large cycles according to a comparison with the SEM images (Fig. 4a and c). This indicates that the superhydrophobic coating displays good mechanical stability.

Importantly, the bending experiment was performed as well to investigate the above-mentioned mechanical stability (Movie S2, Movie S3). A bending experiment was carried out, and then, the corresponding water contact angle was recorded every 30° bending of the coating. As shown in Fig. 4, the coating could maintain its superhydrophobic property after every bending increment. Obviously, the CA reached its maximum value (153°), which illustrated that the coating exhibited excellent mechanical stability and durability. The main reason is that the coating benefits from the epoxy resin, which enhanced the adhesive force between the superhydrophobic powder and the substrate. This innovative method successfully proves the mechanical stability as well, which is suitable for composite insulators with wide application prospects.

3.3. Chemical and environmental durability

For practical applications, a composite insulator is required to work under different extreme conditions such as industrial pollution, hostile environments and UV radiation areas [28]. UV-light exposure treatment, a pH test and an environment durability test were carried out to evaluate the chemical and environmental durability of the prepared superhydrophobic coating.

Consequently, a simple UV-durability test was conducted by irradiation using an artificial light source (20 W, 254 nm). As exhibited in Fig. 5Aa, the coating (5 cm × 2 cm) was exposed to UV light for 24 h, and the wetting behaviour was measured from 0 to 24 h. It is worth nothing that the CA decreased to 151° when the exposure time increased to 12 h. When the exposure time reached 24 h, the coating still maintains its superhydrophobic property. The element Mg decreased from 10.62% to 8.94%, while the element C decreased from 49.74% to 40.43% (Fig. 5Ab), implying that the surface was modified by STA along with the decomposition of $CH_3(CH_2)_{16}COOMg$ under the UV-light exposure. In addition, the intensity of the UV light used was approximately 2% that of sunlight. Therefore, the UV-durability test under UV radiation areas is more meaningful.

In addition, the acidic or alkaline liquid produced by industrial pollution can influence the chemical durability of composite insulators. The coating (5 cm × 2 cm) was immersed into acidic and basic aqueous solutions with different pH values varying from 2 to 14. As shown in Fig. 5B, the $Mg(OH)_2$/epoxy resin superhydrophobic coating was not sensitive to them, and the CAs under strong acidic and alkaline conditions were all above 150°, which exhibits great acid and alkali repellence, thus allowing it to be applied to composite insulators for

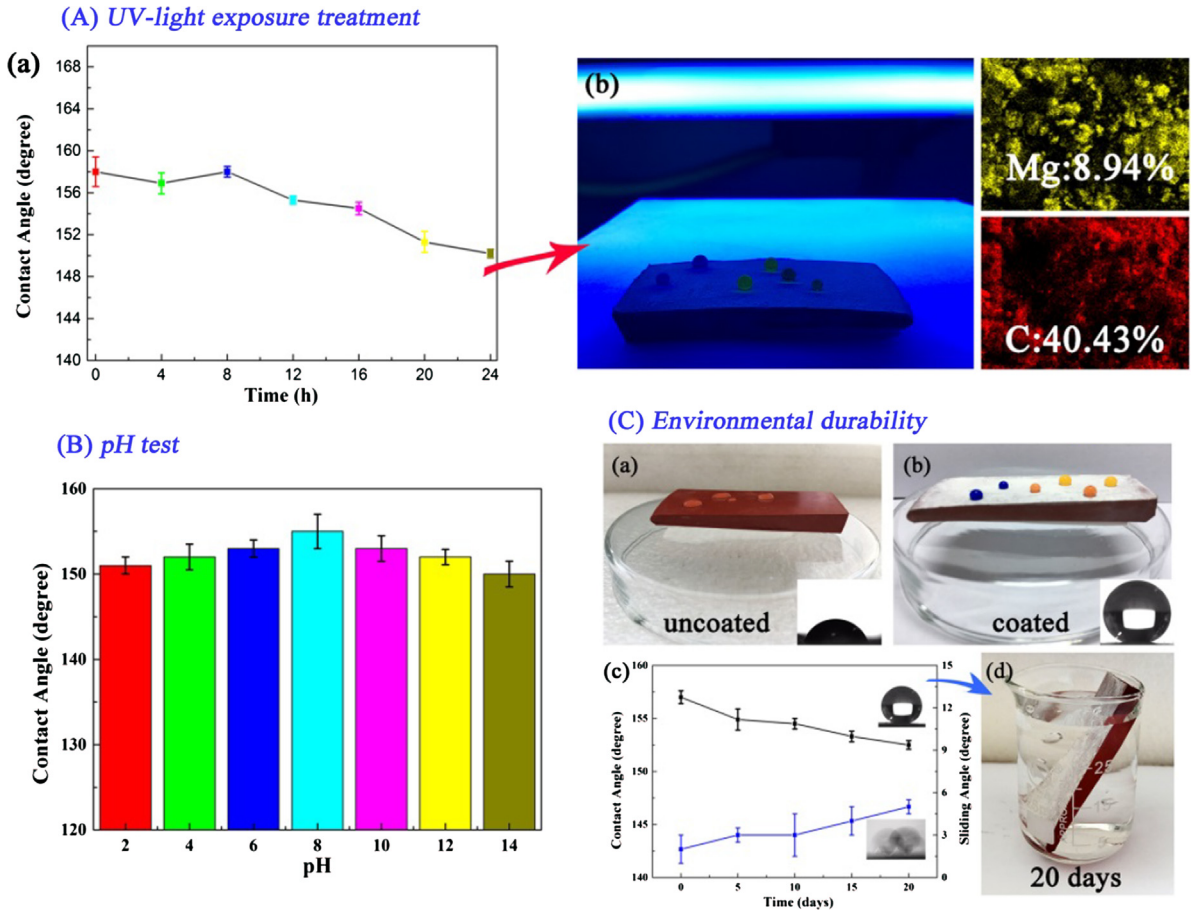

Fig. 5. Chemical and environmental durability measurements. (a) The UV-light exposure treatment. (b) Column charts of the CAs of acidic and basic aqueous solutions with different pH values varying from 2 to 14 on the superhydrophobic coating. (c) Environmental durability.

telecommunication systems.

To explore the environmental durability of the superhydrophobicity of the $Mg(OH)_2$ coating applied to composite insulators, the CAs after different days were measured. As presented in Fig. 5C, the coating was immersed in water for 20 days, and the wetting behaviour was measured every 5 days. The average contact angle and sliding angle were obtained by measuring the same sample at three different sites. The results show that all of the contact angles were larger than 150° and the sliding angles were less than 5°, which can satisfy the requirements of hostile environments.

3.4. Self-cleaning and antifouling properties

Generally speaking, self-cleaning and antifouling properties indicate the ability to self-repel contamination, and these have developed rapidly in recent years [29–33]. Self-cleaning and antifouling abilities can be regarded as important properties of surfaces, which can characterize the superhydrophobicity [34,35]. However, composite insulators could suffer from dust storms and dirty pollution when used in high altitude areas.

In this study, the self-cleaning property and antifouling property of the $Mg(OH)_2$/epoxy resin superhydrophobic coating are shown in Fig. 6. Some sand and dust were spread randomly on the coating and then clean water was poured on it. The result showed that the sand and dust washed away easily (Movie S4). Similarly, muddy water was poured on the coating directly, and it flowed away without residue (Fig. 6b). The self-cleaning and antifouling properties are of great significance because they can keep the composite insulators clean in dirty environments thanks to their great superhydrophobicity.

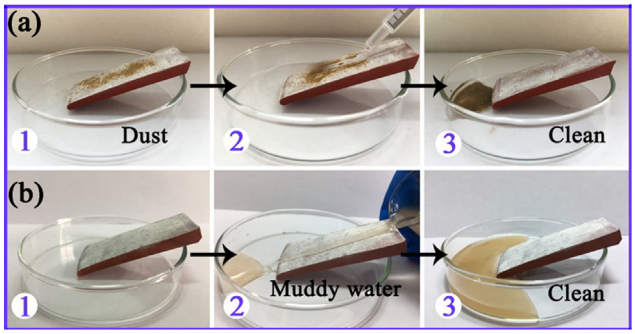

Fig. 6. Self-cleaning property (a) and antifouling ability (b) of the $Mg(OH)_2$/epoxy resin superhydrophobic coating.

3.5. Anti-icing ability

It is well known that ice accumulation on composite insulators can seriously threaten the safe operation of electricity, railways, telecommunication systems and networks, all of which can cause irretrievable losses and catastrophic affairs [36–40].

Herein, an anti-icing test on the $Mg(OH)_2$/epoxy resin superhydrophobic coating is displayed in Fig. 7. Both coated composite insulators and uncoated composite insulators were placed in a temperature of −10 °C with a water droplet (~40 μL) dripped on each sample. First, the water can roll down the coated surface. As time went by, the coated composite insulators still retained their superhydrophobicity for 450 s, while the uncoated composite insulators completely froze (Fig. 7b). However, the water droplet on the coated composite

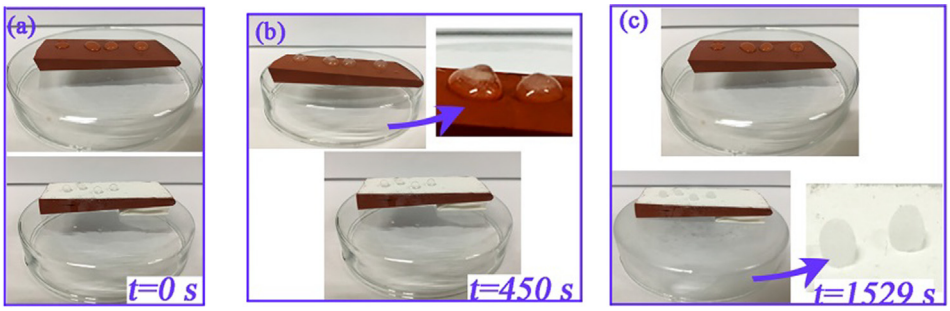

Fig. 7. Photographs of the anti-icing test of the uncoated and coated composite insulator.

insulators froze completely at approximately 1529 s, which can delay the icing time. The phenomenon that spheroidal ice can be easily removed without any force proved that the surface had low adhesion. Hence, the coating can protect composite insulators from freezing disasters in some extreme climates.

3.6. Anti-voltage ability

Almost all composite insulators are placed in long-distance transmission lines to resist huge voltage. It is essential to fabricate a special coating for a composite insulator that possesses both waterproof and anti-voltage properties. Therefore, special attention is paid to anti-voltage strategies regarding decreasing the voltage and delaying the outage time [1,41,42].

The anti-voltage activities of uncoated composite insulators and coated composite insulators through the experimental table are presented by the performance of the anti-voltage test. Here, the anti-voltage ability of the $Mg(OH)_2$/epoxy resin superhydrophobic coating is displayed in Fig. 8. The experimental facility includes the console, transformer, voltage divider and experimental table (Fig. 8B). The coated composite insulators were placed under different voltages (2 kV, 4 kV, 6 kV, 8 kV, and 10 kV) for 0.5 h. There is no change to the coated composite insulators before and after the voltage increased from 2 kV to 8 kV. However, both uncoated composite insulators and coated composite insulators were placed under 10 kV. After only 5 s, the uncoated composite insulator was mostly burned out and electric sparks appeared; meanwhile, the coated composite insulator retained its superhydrophobicity. However, the process for the formation of an electric spark on the coated composite insulator took approximately 270 s. It is worth mentioning that the element Mg decreased from 10.62% to 10.34%, while the element C decreased from 49.74% to 49.1% after high voltage. This proved that the modified surface remained stable and the specific structure could provide resistance to high voltage. The main reason is that the reduction of space charge leads to the improvement of the hydrophobicity of coated composite insulators. The fabricated anti-voltage surface remains meaningful and practical for applications of composite insulators in the global energy field and economy.

4. Conclusions

In summary, an immersion method for fabricating a $Mg(OH)_2$/epoxy resin superhydrophobic coating applied to composite insulators was successfully employed in this paper. The water contact angle and the roughness of surface depend on the STA loading, as shown in SEM and TEM images. The as-prepared coating not only presents water contact angles larger than 150° and sliding angles less than 5° but also

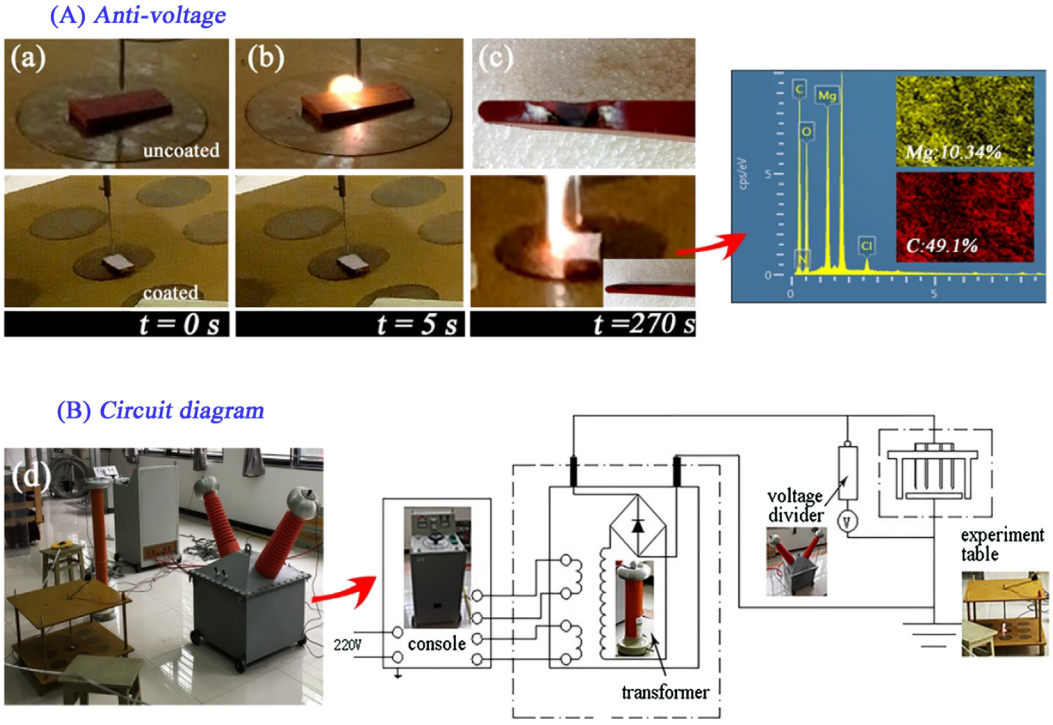

Fig. 8. (A) Photographs of the anti-voltage test of uncoated and coated composite insulators. (B) Photographs of the circuit diagram.

exhibits low adhesion between the covered powders and the surface. Moreover, the sandpaper-abrasion test and bending experiment verify the excellent mechanical stability of the coating. This type of multi-functional composite insulator can maintain its superhydrophobicity after strong UV light treatment and different acid or alkaline tests. Taking practical applications and simple methods into account, the Mg $(OH)_2$/epoxy resin superhydrophobic coating has a promising application value in many fields, such as railways, electricity and telecommunication systems, which is of great significance to global electricity issues and economy development.

Acknowledgements

This work is supported by the National Natural Science Foundation of China (NO. 51475264, 51605254, and 51522510), the National United Engineering Laboratory for Advanced Bearing Tribology, Henan University of Science and Technology, 201710, and the Natural Science Foundation of Hubei Province (No. 2016CFB565). It was sponsored by the Research Fund for Excellent Dissertation of China Three Gorges University (2018SSPY045).

Appendix A. Supplementary material

Supplementary data to this article can be found online at https://doi.org/10.1016/j.apsusc.2018.10.039.

References

[1] M. Liang, K.L. Wong, Improving the long-term performance of composite insulators use nanocomposite: a review, Energy Procedia. 110 (2017) 168–173.
[2] M. Kumosa, Y. Han, L. Kumosa, Analyses of composite insulators with crimped end-fittings: Part I non linear finite element computations, Compos. Sci. Technol. 62 (2002) 1191–1207.
[3] S. Khorsand, K. Raeissi, F. Ashrafizadeh, M.A. Arenas, A. Conde, Corrosion behaviour of super-hydrophobic electrodeposited nickel–cobalt alloy film, Appl. Surf. Sci. 364 (2016) 349–357.
[4] N.M. Valipour, F.C. Birjandi, J. Sargolzaei, Super-non-wettable surfaces: a review, Colloids Surf. A 448 (2014) 93–106.
[5] Y.F. Si, Z.G. Guo, Superhydrophobic nanocoatings: from materials to fabrications and to applications, Nanoscale 7 (2015) 5922–5946.
[6] Y.P. Tang, X. Xu, H.Z. Cao, Research progress in preparation technology of micro-nano structural superhydrophobic materials, Mater. Rev. 11 (2012) 014.
[7] J.J. Fu, T. Chen, M.D. Wang, N.W. Yang, S.N. Li, Y. Wang, X.D. Liu, Acid and alkaline dual stimuli-responsive mechanized hollow mesoporous silica nanoparticles as smart nanocontainers for intelligent anticorrosion coatings, ACS Nano 7 (2013) 11397–11408.
[8] Y.F. Si, H. Zhu, L.W. Chen, T. Jiang, Z.G. Guo, A multifunctional transparent superhydrophobic gel nanocoating with self-healing properties, Chem. Commun. 51 (2015) 16794–16797.
[9] B. Bhushan, Y.C. Jung, Natural and biomimetic artificial surfaces for superhydrophobicity, self-cleaning, low adhesion, and drag reduction, Prog. Mater. Sci. 1 (2011) 1–108.
[10] L.J. Zhang, C.F. Guerrero-Juarez, T. Hata, S.P. Bapat, R. Ramos, M.V. Plikus, R.L. Gallo, Dermal adipocytes protect against invasive staphylococcus aureus skin infection, Science 347 (2015) 67–71.
[11] L.W. Chen, Z.G. Guo, W.M. Liu, Biomimetic multi-functional superamphiphobic FOTS-TiO_2 particles beyond lotus leaf, ACS Appl. Mater. Interf. 8 (2016) 27188–27198.
[12] L. Wang, J. Yang, Y. Zhu, Z. Li, T. Shen, D.Q. Yang, An environment-friendly fabrication of superhydrophobic surfaces on steel and magnesium alloy, Mater. Lett. 171 (2016) 297–299.
[13] B. Qian, Z. Shen, Fabrication of superhydrophobic surfaces by dislocation-selective chemical etching on aluminum, copper, and zinc substrates, Langmuir 21 (2005) 9007–9009.
[14] X. Deng, L. Mammen, H.J. Butt, D. Vollmer, Candle soot as a template for a transparent robust superamphiphobic coating, Science 335 (2012) 67–70.
[15] H. Liu, L. Feng, J. Zhai, L. Jiang, D.B. Zhu, Reversible wettability of a chemical vapor deposition prepared ZnO film between superhydrophobicity and superhydrophilicity, Langmuir 20 (2004) 5659–5661.
[16] Z. Zuo, R. Liao, X. Zhao, et al., Anti-frosting performance of superhydrophobic surface with ZnO nanorods, Appl. Therm. Eng. 110 (2017) 39–48.
[17] H.Q. Cao, H. Zheng, J.F. Yin, Y.X. Lu, S.S. Wu, X.M. Wu, B.J. Li, Mg $(OH)_2$ complex nanostructures with superhydrophobicity and flame retardant effects, J. Phys. Chem. C 114 (41) (2010) 17362–17368.
[18] X.Y. Li, B.B. Yang, Y.Q. Zhang, G.T. Gu, M.M. Li, L.Q. Mao, A study on superhydrophobic coating in anti-icing of glass/porcelain insulator, J. Sol-Gel Sci. Technol. 69 (2) (2014) 441–447.
[19] C.Q. Wang, J.Y. Xiao, J.C. Zeng, D.Z. Jiang, Z.Q. Yuan, A novel method to prepare a microflower-like superhydrophobic epoxy resin surface, Mater. Chem. Phys. 135 (2012) 10–15.
[20] N. Yokoi, K. Manabe, M. Tenjimbayashi, S. Shiratori, Optically transparent superhydrophobic surfaces with enhanced mechanical abrasion resistance enabled by mesh structure, ACS Appl. Mater. Interf. 7 (2015) 4809–4816.
[21] Y.J. Wan, L.C. Tang, D. Yan, L. Zhao, Y.B. Li, L.B. Wu, J.X. Jiang, G.Q. Lai, Improved dispersion and interface in the graphene/epoxy composites via a facile surfactant-assisted process, Compos. Sci. Technol. 82 (2013) 60–68.
[22] Z. Xu, Y. Zhao, H. Wang, H. Zhou, C. Qin, X. Wang, T. Lin, Fluorine-free superhydrophobic coatings with pH-induced wettability transition for controllable oil-water separation, ACS Appl. Mater. Interf. 8 (2016) 5661–5667.
[23] Y.F. Si, Z.Z. Guo, W.W. Liu, A robust epoxy resins @ stearic acid-Mg $(OH)_2$ micronanosheet superhydrophobic omnipotent protective coating for real-life applications, ACS Appl. Mater. Interf. 8 (2016) 16511–16520.
[24] V. Hessel, P. Detemple, J.F. Geiger, M. Keil, R. Schafer, R. Festag, J.H. Wendorff, Low-temperature plasma treatment of magnesium stearate Langmuir-Blodgett films, Thin Solid Films 286 (1-2) (1996) 241–251.
[25] Y. Liang, M.D. Wang, C. Wang, J. Feng, J.S. Li, L.J. Wang, J.J. Fu, Facile synthesis of smart nanocontainers as key components for construction of self-healing coating with superhydrophobic surfaces, Nanoscale Res. Lett. 11 (2016) 231.
[26] W.H. Huang, C.S. Lin, Robust superhydrophobic transparent coatings fabricated by a low-temperature sol–gel process, Appl. Surf. Sci. 305 (2014) 702–709.
[27] X. Men, X. Shi, B. Ge, Y. Li, X. Zhu, Y. Li, Z. Zhang, Novel transparent, liquid-repellent smooth surfaces with mechanical durability, Chem. Eng. J. 296 (2016) 458–465.
[28] R.M.A. Velasquez, J.V.M. Lara, The need of creating a new nominal creep age distance in accordance with heaviest pollution 500 kV overhead line insulators, Eng. Fail. Anal. 86 (2018) 21–32.
[29] W. Yang, J. Li, P. Zhou, L. Zhu, H. Tang, Superhydrophobic copper coating: switchable wettability, on-demand oil-water separation, and antifouling, Chem. Eng. J. 327 (2017) 849–854.
[30] J. Zhang, A. Wang, S. Seeger, Nepenthes pitcher inspired anti-wetting silicone nanofilaments coatings: preparation, unique anti-wetting and self-cleaning behaviors, Adv. Funct. Mater. 24 (2014) 1074–1080.
[31] Y.M. Yang, Fabrication of antireflective self-cleaning surfaces using layer-by-layer assembly techniques, Nanotechnol. Approach (2013) 277–311.
[32] H. Li, S. Yu, X. Han, Fabrication of CuO hierarchical flower-like structures with biomimetic superamphiphobic, self-cleaning and corrosion resistance properties, Chem. Eng. J. 283 (2016) 1443–1454.
[33] K.L. Chen, S.X. Zhou, L.M. Wu, Self-healing underwater superoleophobic and antibiofouling coatings based on the assembly of hierarchical microgel spheres, ACS Nano 10 (2015) 1386–1394.
[34] C. Cao, M. Ge, J. Huang, S. Li, S. Deng, S. Zhang, Z. Chen, K. Zhang, Y. Lai, Robust fluorine-free superhydrophobic PDMS–ormosil @ fabrics for highly effective self-cleaning and efficient oil–water separation, J. Mater. Chem. A 4 (2016) 12179–12187.
[35] J. Chanda, L. Ionov, A. Kirillova, A. Synytska, New insight into icing and de-icing properties of hydrophobic and hydrophilic structured surfaces based on core–shell particles, Soft Matter. 11 (2015) 9126–9134.
[36] Y.H. Yeong, C. Wang, K.J. Wynne, M.C. Gupta, Oil-infused superhydrophobic silicone material for low ice adhesion with long-term infusion stability, ACS Appl. Mater. Interf. 8 (2016) 32050–32059.
[37] C.Q. Wei, B.Y. Jin, Q.H. Zhang, X.L. Zhan, F.Q. Chen, Anti-icing performance of super-wetting surfaces from icing-resistance to ice-phobic aspects: robust hydrophobic or slippery surfaces, Alloys Compd. (2018).
[38] S. Pan, N. Wang, D.S. Xiong, Y.L. Deng, Y. Shi, Fabrication of superhydrophobic coating via spraying method and its applications in anti-icing and anti-corrosion, Appl. Surf. Sci. 389 (2016) 547–553.
[39] C. Tao, S. Bai, X.H. Li, C. Li, L.X. Ren, Y.H. Zhao, X.Y. Yuan, Formation of zwitterionic coatings with an aqueous lubricating layer for antifogging/anti-icing applications, Prog. Org. Coat. 115 (2018) 56–64.
[40] L.L. Cao, A.K. Jones, V.K. Sikka, J.Z. Wu, D. Gao, Anti-icing superhydrophobic coatings, Langmuir 25 (2009) 12444–12448.
[41] S. Ibrahim, M.A. Rehim, G. Turky, Dielectric study of polystyrene/polycaprolactone composites prepared by miniemulsion polymerization, J. Phys. Chem. Solids 119 (2018) 56–61.
[42] W.H. Henley, Y. He, J.S. Mellors, N.G. Batza, J.M. Ramsey, J.W. Jorgenson, High resolution separations of charge variants and disulfide isomers of monoclonal antibodies and antibody drug conjugates using ultra-high voltage capillary electrophoresis with high electric field strength, J. Chromatogr. A 1523 (2017) 72–79.